JHEP

Published for SISSA by Springer

Received: February 12, 2015
Accepted: April 17, 2015
Published: May 7, 2015

Effective theories for dark matter nucleon scattering

Junji Hisano,[a,b,c] **Ryo Nagai**[b] **and Natsumi Nagata**[c,d]

[a] *Kobayashi-Maskawa Institute for the Origin of Particles and the Universe, Nagoya University, Nagoya 464-8602, Japan*

[b] *Department of Physics, Nagoya University, Nagoya 464-8602, Japan*

[c] *Kavli Institute for the Physics and Mathematics of the Universe (WPI), The University of Tokyo Institutes for Advanced Study, The University of Tokyo, Kashiwa, Chiba 277-8583, Japan*

[d] *William I. Fine Theoretical Physics Institute, School of Physics and Astronomy, University of Minnesota, Minneapolis, MN 55455, U.S.A.*

E-mail: hisano@eken.phys.nagoya-u.ac.jp, nagai@th.phys.nagoya-u.ac.jp, nagat006@umn.edu

Abstract: We reformulate the calculation of the dark matter-nucleon scattering cross sections based on the method of effective field theories. We assume that the scatterings are induced by the exchange of colored mediators, and construct the effective theories by integrating out the colored particles. All of the leading order matching conditions as well as the renormalization group equations are presented. We consider a Majorana fermion, and real scalar and vector bosons for the dark matter and show the results for each case. The treatment for the twist-2 operators is discussed in detail, and it is shown that the scale of evaluating their nucleon matrix elements does not have to be the hadronic scale. The effects of the QCD corrections are evaluated on the assumption that the masses of the colored mediators are much heavier than the electroweak scale. Our formulation is systematic and model-independent, and thus suitable to be implemented in numerical packages, such as `micrOMEGAs` and `DarkSUSY`.

Keywords: Beyond Standard Model, Cosmology of Theories beyond the SM

ArXiv ePrint: 1502.02244

Open Access, © The Authors.
Article funded by SCOAP[3].

doi:10.1007/JHEP05(2015)037

JHEP05(2015)037

Contents

JHEP05(2015)037

1 Introduction

Weakly Interacting Massive Particles (WIMPs) have been widely regarded as the most attractive candidate for dark matter (DM) in the Universe. They are weakly coupled to the Standard Model (SM) particles so that they are thermalized in the early Universe. Their relic abundance is determined by their annihilation cross sections, and it turns out that WIMPs may have a correct value of the cross sections to give the observed DM density $\Omega_{\rm DM}h^2 = 0.1196 \pm 0.0031$ [1]. Moreover, such particles are often predicted in new physics beyond the SM. For instance, the lightest neutralino in the minimal supersymmetric Standard Model (MSSM) is a well-know candidate for WIMP DM.

Since WIMPs are interacting with the ordinary matters, it is possible to use these interactions to detect them directly. Experiments based on such a strategy are called the DM direct detection experiments. These experiments search for the scattering signals of WIMPs kicking off target nuclei on the earth by detecting the recoil energy transferred to

the nuclei. At present, the LUX experiment has the best sensitivity, and provides a limit on the spin-independent WIMP-nucleon scattering cross section as $\sigma_{\rm SI} < 7.6 \times 10^{-46}$ cm^2 at a mass of 33 GeV [2]. Further, there exist several proposals with ton-scale detectors, which will offer extremely improved sensitivities.

To study the properties of WIMPs based on the direct detection experiments, it is necessary to evaluate the WIMP-nucleus scattering cross sections accurately. The interactions of a WIMP with a nucleon, as well as a nucleus, are generated through the couplings of the WIMP with quarks and gluons. These couplings are described in terms of the parton-level interactions, and contribute to the interactions with a nucleon through non-perturbative QCD effects. An appropriate way to compute the contribution is to take an effective theoretical approach. Here, the parton-level interactions are expressed by the higher-dimensional operators, and their contribution to the WIMP-nucleon couplings is computed by means of their nucleon matrix elements. See refs. [3, 4] for the treatments.

Usually, the parton-level interactions are mediated by heavy particles. Since the WIMPs are singlet with respect to the $\mathrm{SU(3)_C \otimes U(1)_{EM}}$ symmetry, the particles mediating the WIMP-quark interactions should be also electrically neutral and color singlet when they are exchanged in the t-channel, while they should be charged and colored when they are exchanged in the s- or u-channel. The extent of the significance of these contributions highly depends on models. For example, in the case of the neutralino DM in the MSSM, the Z boson and the Higgs boson mediating processes are classified into the former type, while the squark exchange is the latter one. When squarks are extremely heavy, only the former contribution is sizable. In the limit of pure gaugino or higgsino case, on the other hand, the former contribution vanishes and thus the latter may be dominant. Therefore, it is desirable to construct a formalism to evaluate all of the contributions precisely enough on an equal footing.

Recently, the LHC experiments give stringent limits on the masses of new colored particles. The results may suggest that the colored mediators which induce the couplings of WIMPs with quarks and gluon, if they exist, should have masses much heavier than $\sim$ 100 GeV. In this case, the contribution of such a particle to the WIMP-nucleon interaction receives sizable QCD corrections because of the mass hierarchy and the large value of the strong coupling constant. This motivates us to reformulate the calculation in the following way; first, we obtain the effective theory which consists of the higher dimensional operators of DM and quarks/gluons at the energy scale of the mediator mass. At this point, we need to match the effective theory to the full theory so that only the short-distance contribution is to be included in the Wilson coefficients of the higher-dimensional operators. Then, we evolve the operators by using the renormalization group equations (RGEs) down to the scale at which the nucleon matrix elements of the operators are evaluated. It is the prescription that we will discuss in this paper. We will formulate a complete framework to carry out the calculation to the leading order in the strong coupling constant. In this formulation, all of the model dependence is included into the Wilson coefficients of the effective operators, and the rest part of the steps is independent of models. Therefore, the method is quite suitable for generic computational codes such as `micrOMEGAs` [5] or `DarkSUSY` [6].

JHEP05(2015)037

In addition, we will discuss in detail the treatment for the twist-2 operators and show that we do not have to evolve the operators down to the hadronic scale ($\sim 1\,\mathrm{GeV}$); we may evaluate their nucleon matrix elements around the electroweak scale. This point is often misunderstood, and we believe that our analysis clarifies the confusion. Furthermore, we will show the significance of the renormalization effects on the operators when the masses of the colored mediators are much heavier than the electroweak scale.

This paper is organized as follows. In section 2, we discuss our formulation in the case where DM is a Majorana fermion. We present the effective operators for the Majorana fermion and evaluate the matching conditions on their Wilson coefficients. The RGEs of the operators are listed there as well. The results for the real scalar and vector boson DM cases are also given in section 3 and section 4, respectively. Then, in section 5, we study the renormalization effects by using a particular model. Also, we will discuss the treatment of the twist-2 operators in the section. Section 6 is devoted to conclusion. In appendix, we present the formulae for the one-loop contribution to the scalar-type gluon operators in the case of scalar DM, which as far as we know have not been given in the literature so far. The result is useful when the colored mediators have masses around the electroweak scale.

2 Formalism: Majorana fermion DM

In this section, we give a formalism to evaluate the scattering cross sections of a WIMP with a nucleon. The procedure described here consists of the following steps. First, we construct the effective theory for the WIMP, quarks, and gluons, by integrating out the mediator particles. The effective interactions obtained here are expressed in terms of the higher-dimensional operators. Then, we evolve the Wilson coefficients of the effective operators according to the RGEs down to the scale at which the nucleon matrix elements of the operators are evaluated. Finally, we express the effective coupling of the WIMP with a nucleon in terms of the Wilson coefficients and the nucleon matrix elements. The scattering cross sections are readily obtained from the effective coupling. We will evaluate them to the leading order in the strong coupling constant throughout this work.

In this section, we assume that the WIMP DM to be a Majorana fermion. The real scalar boson DM and the real vector boson DM cases are discussed in section 3 and section 4, respectively. It should be noted that Dirac fermion and complex scalar DM candidates are severely constrained by the DM direct detection experiments because they in general couple to the vector current of quark fields. Furthermore, this vector interaction is not renormalized, and thus the conventional way of calculation is sufficient for this contribution [7]. For these reasons, we do not consider these cases in this paper.

2.1 Effective Lagrangian

To begin with, let us write down the effective interactions of a Majorana fermion, which is assumed to be a WIMP, with quarks and gluon. The interactions are expressed in terms of the following higher-dimensional operators [3]:

$$\mathcal{L}_{\mathrm{eff}} = \sum_{p=q,g} C_S^p \mathcal{O}_S^p + \sum_{i=1,2} \sum_{p=q,g} C_{T_i}^p \mathcal{O}_{T_i}^p + \sum_q C_{AV}^q \mathcal{O}_{AV}^q \,, \tag{2.1}$$

JHEP05(2015)037

with

$$\begin{aligned}
\mathcal{O}_S^q &\equiv \overline{\widetilde{\chi}^0}\widetilde{\chi}^0 m_q \bar{q} q \,, \\
\mathcal{O}_S^g &\equiv \frac{\alpha_s}{\pi}\overline{\widetilde{\chi}^0}\widetilde{\chi}^0 G^A_{\mu\nu} G^{A\mu\nu} \,, \\
\mathcal{O}_{T_1}^p &\equiv \frac{1}{M}\overline{\widetilde{\chi}^0} i\partial^\mu \gamma^\nu \widetilde{\chi}^0 \mathcal{O}^p_{\mu\nu} \,, \\
\mathcal{O}_{T_2}^p &\equiv \frac{1}{M^2}\overline{\widetilde{\chi}^0} i\partial^\mu i\partial^\nu \widetilde{\chi}^0 \mathcal{O}^p_{\mu\nu} \,, \\
\mathcal{O}_{AV}^q &\equiv \overline{\widetilde{\chi}^0}\gamma_\mu\gamma_5\widetilde{\chi}^0 \bar{q}\gamma^\mu\gamma_5 q \,.
\end{aligned} \tag{2.2}$$

Here, we only keep the operators that remain sizable in the non-relativistic limit. In addition, we have used the classical equations of motion and the integration by parts to drop the redundant operators [8, 9]. $\widetilde{\chi}^0$, q, and $G^A_{\mu\nu}$ denote the Majorana fermion, quarks ($q = u, d, s, c, b, t$), and the field strength tensor of gluon field, respectively; m_q are the masses of quarks; M is the mass of the WIMP; $\alpha_s \equiv g_s^2/(4\pi)$ is the strong coupling constant, $\mathcal{O}^q_{\mu\nu}$ and $\mathcal{O}^g_{\mu\nu}$ are the twist-2 operators of quarks and gluon, respectively, which are defined by[1]

$$\begin{aligned}
\mathcal{O}^q_{\mu\nu} &\equiv \frac{1}{2}\bar{q} i\left(D_\mu\gamma_\nu + D_\nu\gamma_\mu - \frac{1}{2}g_{\mu\nu}\not{D}\right) q \,, \\
\mathcal{O}^g_{\mu\nu} &\equiv G^{A\rho}_\mu G^A_{\nu\rho} - \frac{1}{4} g_{\mu\nu} G^A_{\rho\sigma} G^{A\rho\sigma} \,,
\end{aligned} \tag{2.3}$$

with D_μ the covariant derivatives. The effective operators are defined at the mass scale of mediators, which is assumed to be well above the mass of top quark. Generalization to other cases is straightforward; for instance, if such heavy particles have masses similar to or lighter than the top mass, one should integrate top quark as well so that the effective theoretical approach is appropriate.[2]

Note that we include α_s/π to the definition of the gluon scalar-type operator $\mathcal{O}^g_S$. We discuss the meaning in the next subsection.

2.2 Nucleon matrix elements

As discussed in Introduction, we need the nucleon matrix elements of the effective operators to evaluate the WIMP-nucleon effective coupling. These operators are classified into three types in terms of the Lorentz transformation properties of the quark bilinear parts in the operators; the scalar-type operators ($\mathcal{O}^q_S$, $\mathcal{O}^g_S$), the axial-vector operator ($\mathcal{O}^q_{AV}$), and the twist-2-type operators ($\mathcal{O}^q_{T_i}$, $\mathcal{O}^g_{T_i}$). Since these operators do not mix with each other under the renormalization group (RG) flow, we are allowed to consider them separately.

As for the scalar-type quark operators $\mathcal{O}^q_S$, we use the results from the lattice QCD simulations. The expectation values of the scalar bilinear operators of light quarks between

[1] Notice that we have changed the definition of $\mathcal{O}^g_{\mu\nu}$ by a factor of -1 from those in refs. [3, 4]. We follow the convention used in ref. [10].

[2] In ref. [11], such a situation is discussed where the exchanged particle has a similar mass to the b-quark mass. In this case, of course, b-quark (also top quark) should be simultaneously integrated out when the effective theory is formulated.

JHEP05(2015)037

Proton		Neutron	
$f_{T_u}^{(p)}$	0.019(5)	$f_{T_u}^{(n)}$	0.013(3)
$f_{T_d}^{(p)}$	0.027(6)	$f_{T_d}^{(n)}$	0.040(9)
$f_{T_s}^{(p)}$	0.009(22)	$f_{T_s}^{(n)}$	0.009(22)

Table 1. Mass fractions. These values are based on the lattice QCD simulations [13, 14].

the nucleon states at rest, $|N\rangle$ $(N = p, n)$, are parametrized as

$$f_{T_q}^{(N)} \equiv \langle N|m_q\bar{q}q|N\rangle/m_N\,, \tag{2.4}$$

which are called the mass fractions. These values are shown in table 1. Here, m_N is the nucleon mass. They are taken from ref. [12], in which the mass fractions are computed by using the results from refs. [13, 14].

The nucleon matrix element of $\mathcal{O}_S^g$ is, on the other hand, evaluated with the trace anomaly of the energy-momentum tensor [15]. For $N_f = 3$ quark flavors, the trace of the energy-momentum tensor in QCD is given as

$$\Theta^\mu{}_\mu = -\frac{9}{8}\frac{\alpha_s}{\pi}G^A_{\mu\nu}G^{A\mu\nu} + \sum_{q=u,d,s} m_q\bar{q}q\,, \tag{2.5}$$

up to the leading order in α_s. The relation beyond the leading order in α_s is also readily obtained from the trace-anomaly formula. By evaluating the operator (2.5) in the nucleon states $|N\rangle$, from $\langle N|\Theta^\mu{}_\mu|N\rangle = m_N$ we then obtain

$$\langle N|\frac{\alpha_s}{\pi}G^A_{\mu\nu}G^{A\mu\nu}|N\rangle = -\frac{8}{9}m_N f_{T_G}^{(N)}\,, \tag{2.6}$$

with $f_{T_G}^{(N)} \equiv 1 - \sum_{q=u,d,s} f_{T_q}^{(N)}$. Notice that the r.h.s. of eq. (2.6) is the order of the typical hadronic scale, $\mathcal{O}(m_N)$. That is, although we include a factor of α_s/π in the definition of $\mathcal{O}_S^g$, its nucleon matrix element is not suppressed by α_s/π. This is the reason why we have defined $\mathcal{O}_S^g$ to contain α_s/π.

Next, we discuss the nucleon matrix elements of the twist-2 operators. They are given by the second moments of the parton distribution functions (PDFs):

$$\langle N(p)|\mathcal{O}^q_{\mu\nu}|N(p)\rangle = \frac{1}{m_N}\Big(p_\mu p_\nu - \frac{1}{4}m_N^2 g_{\mu\nu}\Big)(q(2;\mu) + \bar{q}(2;\mu))\,, \tag{2.7}$$

$$\langle N(p)|\mathcal{O}^g_{\mu\nu}|N(p)\rangle = -\frac{1}{m_N}\Big(p_\mu p_\nu - \frac{1}{4}m_N^2 g_{\mu\nu}\Big)g(2;\mu)\ . \tag{2.8}$$

with

$$q(2;\mu) = \int_0^1 dx\ x\ q(x,\mu)\ , \tag{2.9}$$

$$\bar{q}(2;\mu) = \int_0^1 dx\ x\ \bar{q}(x,\mu)\ , \tag{2.10}$$

$$g(2;\mu) = \int_0^1 dx\ x\ g(x,\mu)\ . \tag{2.11}$$

JHEP05(2015)037

$g(2)$	0.464(2)		
$u(2)$	0.223(3)	$\bar{u}(2)$	0.036(2)
$d(2)$	0.118(3)	$\bar{d}(2)$	0.037(3)
$s(2)$	0.0258(4)	$\bar{s}(2)$	0.0258(4)
$c(2)$	0.0187(2)	$\bar{c}(2)$	0.0187(2)
$b(2)$	0.0117(1)	$\bar{b}(2)$	0.0117(1)

Table 2. Second moments of the PDFs of proton evaluated at $\mu = m_Z$. We use the CJ12 next-to-leading order PDFs given by the CTEQ-Jefferson Lab collaboration [16].

Here $q(x,\mu)$, $\bar{q}(x,\mu)$ and $g(x,\mu)$ are the PDFs of quarks, antiquarks and gluon at the factorization scale μ, respectively. These values are well measured at various energy scales, contrary to the case of the scalar matrix elements. In table 2, for example, we present the second moments for proton at the scale of $\mu = m_Z$ with m_Z the Z boson mass. Here, we use the CJ12 next-to-leading order PDFs given by the CTEQ-Jefferson Lab collaboration [16]. Those for neutron are given with the exchange of up and down quarks. As can be seen, the second moment for gluon $g(2;\mu)$ is of the same order of magnitude as those for quarks. As a result, the nucleon matrix element of the gluon twist-2 tensor in eq. (2.8) is $\mathcal{O}(m_N)$. This justifies the definition of $\mathcal{O}^g_{T_i}$, where we have not included a factor of α_s/π in this case. Our definition for the gluonic operators ($\mathcal{O}^g_S$, and $\mathcal{O}^g_{T_i}$) clarifies the order counting with respect to α_s/π.

Finally, the nucleon matrix elements of the axial vector-type operators are given by

$$\langle N|\bar{q}\gamma_\mu\gamma_5 q|N\rangle = 2s_\mu \Delta q_N \ . \tag{2.12}$$

with Δq_N called the spin fractions and s_μ being the spin of the nucleon. The values of the spin fractions are taken from ref. [17]; $\Delta u_p = 0.77$, $\Delta d_p = -0.49$, and $\Delta s_p = -0.15$ for proton. Those of neutron are to be obtained by exchanging the values of up and down quarks.

2.3 Wilson coefficients

Next, we evaluate the Wilson coefficients of the effective operators by integrating out heavy mediator particles. Here, we consider a generic situation in which the interaction Lagrangian of the Majorana fermion with quarks is given by

$$\mathcal{L}_{\rm int} = \overline{q}(a_q + b_q\gamma_5)\widetilde{\chi}^0\widetilde{q} \ + \ \text{h.c.}\,, \tag{2.13}$$

where $\widetilde{q}$ denotes a heavy, colored scalar particle with its mass represented by $M_{\widetilde{q}}$.

The interaction gives rise to the coupling of the Majorana fermion with quarks via the tree-level exchange of the colored mediator. By evaluating the diagram, we readily obtain the Wilson coefficients of the effective operators containing quarks. The matching

JHEP05(2015)037

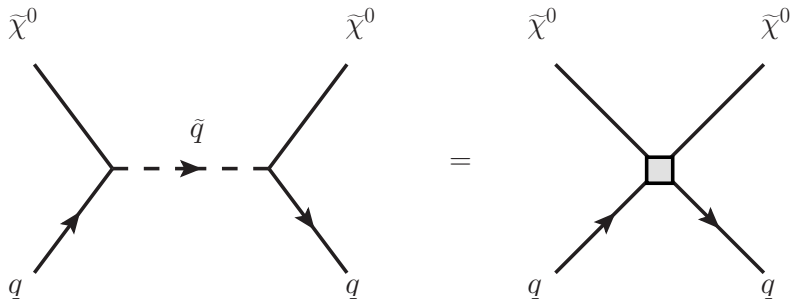

Figure 1. Tree-level matching condition for Majorana fermion-quark effective interactions. Gray square represents the vertex for the quark effective operators.

procedure is illustrated in figure 1. Here, the gray square represents the vertex for the WIMP-quark effective operators. As a result, we have

$$\begin{aligned} C_S^q(\mu_F) &= \frac{a_q^2+b_q^2}{8}\frac{M}{(M_{\tilde{q}}^2-M^2)^2} - \frac{a_q^2-b_q^2}{4m_q}\frac{1}{M_{\tilde{q}}^2-M^2}\,, \\ C_{T_1}^q(\mu_F) &= \frac{a_q^2+b_q^2}{2}\frac{M}{(M_{\tilde{q}}^2-M^2)^2}\,, \\ C_{T_2}^q(\mu_F) &= 0\,, \\ C_{AV}^q(\mu_F) &= \frac{a_q^2+b_q^2}{4}\frac{1}{M_{\tilde{q}}^2-M^2}\,. \end{aligned} \tag{2.14}$$

Here, μ_F denotes the factorization scale, which is taken to be the mass scale of exchanged scalar particles. We have performed the expansion in terms of the quark momenta; i.e., this calculation is valid when $(p\cdot q)/(M_{\tilde{q}}^2-M^2) \ll 1$ with p_μ and q_μ being the momenta of DM and quarks, respectively (See also footnote 2).[3]

Next, we derive the matching condition for the WIMP-gluon effective operators. At this point, we need to include only the short-distance contribution to the Wilson coefficients [4, 19]. This is achieved by the matching procedure shown in figure 2. This reads

$$\begin{aligned} C_S^g(\mu_F) &= -\sum_q \frac{M(a_q^2+b_q^2)}{96M_{\tilde{q}}^2(M_{\tilde{q}}^2-M^2)}\,, \\ C_{T_i}^g(\mu_F) &= 0\,. \end{aligned} \tag{2.15}$$

Here, the summation is taken over all quark flavors. Note that the Wilson coefficient of the gluon scalar operator is generated at the leading order in α_s, i.e., $\mathcal{O}(\alpha_s^0)$, while those of the gluon twist-2 operators vanish at this order [4]. They are induced at $\mathcal{O}(\alpha_s)$.

2.4 Renormalization group equations

The effective operators obtained above are evolved by means of RGEs. In this section, we list the RGEs for the operators which we use in the following analysis. In this paper,

[3] On the other hand, it turns out that the WIMP-nucleon scattering cross sections are considerably enhanced when $M_{\tilde{q}} - M < 100$ GeV [18].

JHEP05(2015)037

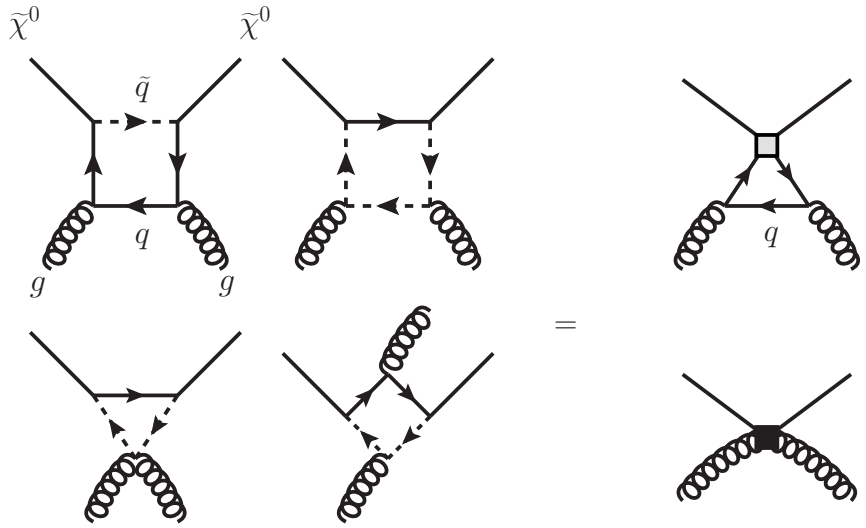

Figure 2. One-loop matching condition for Majorana fermion-gluon effective interactions. Black square represents the vertex for the gluon effective operators.

we only use the one-loop RGEs since our main concern is to formulate the procedure for the leading-order calculation in α_s. For the sake of convenience, however, we also mention some results that may be used for the higher-order calculation.[4]

The one-loop beta function of the strong gauge coupling constant is given by

$$\mu\frac{d\alpha_s}{d\mu} \equiv \beta(\alpha_s) = \frac{\alpha_s^2}{2\pi}\left(-\frac{11}{3}N_c + \frac{2}{3}N_f\right), \tag{2.16}$$

where $N_c = 3$ is the number of colors and N_f denotes the number of quark flavors in an effective theory. Higher-order contribution is found in refs. [22, 23].

Now we give the RGEs for the Wilson coefficients of the above operators. First, we consider the RGEs for the scalar-type operators $(\mathcal{O}_S^q, \mathcal{O}_S^g)$. To that end, notice that the quark mass operator is RG invariant in a mass-independent renormalization scheme like the $\overline{\text{MS}}$ scheme, i.e.,

$$\mu\frac{d}{d\mu}m_q\bar{q}q = 0\ . \tag{2.17}$$

Then, by differentiating the trace anomaly formula (2.5), we also find

$$\mu\frac{d}{d\mu}\frac{\alpha_s}{\pi}G^A_{\mu\nu}G^{A\mu\nu} = 0\,, \tag{2.18}$$

as eq. (2.5) is an operator equation and thus scale-invariant. Accordingly, the scalar-type operators are RG invariant at $\mathcal{O}(\alpha_s)$. This is another reason why we include a factor of α_s in the definition of $\mathcal{O}_S^g$. Beyond the leading order, the scalar-type gluon operator runs and mixes with the scalar-type quark operators during the RG flow. The RGEs for the case are obtained again by using the trace-anomaly formula with the use of the higher-order

[4]See also refs. [20, 21] for relevant discussion.

JHEP05(2015)037

beta function of the gauge coupling constant [22, 23] and anomalous dimensions for quark masses [24, 25].

Next, we consider the RGEs for the twist-2 operators $(O^q_{T_i}, O^g_{T_i})$. The one-loop anomalous dimension matrix of the operators is evaluated as [26]

$$\mu\frac{d}{d\mu}(C^q_{T_i}, C^g_{T_i}) = (C^q_{T_i}, C^g_{T_i})\ \Gamma_T\,, \tag{2.19}$$

with Γ_T a $(N_f+1)\times(N_f+1)$ matrix:

$$\Gamma_T = \frac{\alpha_s}{4\pi}\begin{pmatrix} \frac{16}{3}C_F & 0 & \cdots & 0 & \frac{4}{3} \\ 0 & \frac{16}{3}C_F & & \vdots & \vdots \\ \vdots & & \ddots & 0 & \vdots \\ 0 & \cdots & 0 & \frac{16}{3}C_F & \frac{4}{3} \\ \frac{16}{3}C_F & \cdots & \cdots & \frac{16}{3}C_F & \frac{4}{3}N_f \end{pmatrix}, \tag{2.20}$$

where $C_F = 4/3$ is the quadratic Casimir invariant. Higher order RGEs are found in ref. [27].

Finally, the RGE for the axial-vector interaction is readily obtained since at the leading order the axial-vector current is conserved:

$$\mu\frac{d}{d\mu}C^q_{AV} = 0\,. \tag{2.21}$$

For higher-order corrections, see ref. [28].

2.5 Quark threshold matching

During the RG flow, another matching procedure is required when one goes across a quark threshold. For instance, around the t-quark mass threshold $\mu_t \simeq m_t$, the Wilson coefficients are matched as

$$\begin{aligned}
C^q_S(\mu_t)|_{N_f=5} &= C^q_S(\mu_t)|_{N_f=6}\,, \\
C^g_S(\mu_t)|_{N_f=5} &= -\frac{1}{12}\left[1+\frac{11}{4\pi}\alpha_s(\mu_t)\right]C^t_S(\mu_t)|_{N_f=6} + C^g_S(\mu_t)|_{N_f=6}\,, \\
C^q_{T_i}(\mu_t)|_{N_f=5} &= C^q_{T_i}(\mu_t)|_{N_f=6}\,, \\
C^g_{T_i}(\mu_t)|_{N_f=5} &= C^g_{T_i}(\mu_t)|_{N_f=6}\,, \\
C^q_{AV}(\mu_t)|_{N_f=5} &= C^q_{AV}(\mu_t)|_{N_f=6}\,,
\end{aligned} \tag{2.22}$$

with $q = u, d, s, c, b$. Notice that although we consider the leading-order calculation, we include the next-to-leading order constant contribution to C^g_S here, since the effect is known to be large [29]. Similar matching should be carried out at the b- and c-quark threshold scales, if the coefficients are evolved down below them.

JHEP05(2015)037

In addition, at the threshold scales, the higher-dimensional operators suppressed by a power of the corresponding quark masses may also be generated. For example, at a heavy quark mass threshold m_Q, the $m_Q\overline{Q}Q$ operator gives rise to not only the scalar-type gluon operator $-\alpha_s(m_Q)G^A_{\mu\nu}G^{A\mu\nu}/(12\pi)$, but also the following dimension-six operators [30, 31]:

$$-\frac{\alpha_s(m_Q)}{60\pi m_Q^2}(D^\nu G^A_{\nu\mu})(D^\rho G^A_{\rho\mu}) - \frac{g_s\alpha_s(m_Q)}{720\pi m_Q^2} f_{ABC}G^A_{\mu\nu}G^{B\mu\rho}G^C_{\nu\rho}\,, \tag{2.23}$$

with f_{ABC} the structure constant of $\mathrm{SU}(3)_\mathrm{C}$. Among them, those induced at the charm quark threshold may yield a significant effect. The naive dimensional analysis tells us that the higher dimensional operator (2.23) might give a correction up to $\Lambda^2_\mathrm{QCD}/m_c^2 \simeq 10\%$ to the leading term, though the correction may be parametrically suppressed to a few % by the prefactors of those operators.

At present, there is no way to estimate the contribution of the higher-dimensional operators more accurately. Thus, it should be considered as a theoretical uncertainty of the computation. One way to reduce the uncertainty is to use the nucleon matrix elements evaluated above the charm threshold. As will be discussed in section 5, for the twist-2 operators, it is possible to use the PDFs evaluated above the charm/bottom threshold. For the scalar-type operators, on the other hand, the present lattice simulations are not able to precisely evaluate the charm-quark matrix element [32]. Future simulations may compute it with sufficient accuracy and help to reduce the theoretical uncertainty.

2.6 Scattering cross sections

Finally, we obtain the effective coupling of the Majorana fermion with a nucleon. For the spin-independent coupling, we have

$$\mathcal{L}^{(N)}_\mathrm{SI} = f_N\overline{\widetilde{\chi}^0}\widetilde{\chi}^0\overline{N}N\,, \tag{2.24}$$

where N denotes the nucleon field and

$$\begin{aligned} f_N/m_N = &\sum_{q=u,d,s} C^q_S(\mu_\mathrm{had})f^{(N)}_{T_q} - \frac{8}{9}C^g_S(\mu_\mathrm{had})f^{(N)}_{T_G} \\ &+ \frac{3}{4}\sum_q^{N_f}\sum_{i=1,2} C^q_{T_i}(\mu)[q(2;\mu)+\overline{q}(2;\mu)] - \frac{3}{4}\sum_{i=1,2} C^g_{T_i}(\mu)g(2;\mu)\,, \end{aligned} \tag{2.25}$$

where μ_had is the hadron scale usually taken to be around 1 GeV. For the contribution of the twist-2 operators, the summation runs over the number of the active quark flavors in the effective theory at the energy scale of μ where their nucleon matrix elements are evaluated. As will be shown in section 5, the scale μ does not need to be taken at the hadronic scale; it is allowed to be set around the electroweak scale as long as the PDFs of the scale are known.

The spin-dependent effective coupling is, on the other hand, given by

$$\mathcal{L}^{(N)}_\mathrm{SD} = a_N\overline{\widetilde{\chi}^0}\gamma^\mu\gamma_5\widetilde{\chi}^0\overline{N}\gamma_\mu\gamma_5 N\,, \tag{2.26}$$

JHEP05(2015)037

with

$$a_N = \sum_{q=u,d,s} C_{AV}^q \Delta q_N \ . \tag{2.27}$$

By using the effective couplings, we finally obtain the scattering cross section of the Majorana fermion with a target nucleus as follows:

$$\sigma = \frac{4}{\pi}\left(\frac{MM_T}{M+M_T}\right)^2 \left[|n_p f_p + n_n f_n|^2 + 4\frac{J+1}{J}|a_p\langle s_p\rangle + a_n\langle s_n\rangle|^2\right], \tag{2.28}$$

where M_T is the mass of the target nucleus; n_p and n_n are the numbers of protons and neutrons in the nucleus, respectively; J is the total spin of the nucleus, and $\langle s_N\rangle$ is the expectation value of the spin of a nucleon in the target. Here, we calculate WIMP-nucleus scattering cross sections in the limit of zero momentum transfer, for which each WIMP-nucleon scattering amplitude adds up coherently [7].

3 Formalism: real scalar boson DM

Next we briefly show the results for the case of real scalar boson DM. We may use a similar procedure to that given in the previous section to formulate effective theories for the WIMP.

3.1 Effective Lagrangian

The effective interactions of the real scalar ϕ with quarks and gluon are expressed by

$$\mathcal{L}_{\rm eff} = \sum_{p=q,g} C_S^p \mathcal{O}_S^p + \sum_{p=q,g} C_{T_2}^p \mathcal{O}_{T_2}^p \,, \tag{3.1}$$

with

$$\begin{aligned}
\mathcal{O}_S^q &\equiv \phi^2 m_q \bar{q} q \,, \\
\mathcal{O}_S^g &\equiv \frac{\alpha_s}{\pi}\phi^2 G^{A\mu\nu} G^A_{\mu\nu} \,, \\
\mathcal{O}_{T_2}^q &\equiv \frac{1}{M^2}\phi i\partial^\mu i\partial^\nu \phi \mathcal{O}^q_{\mu\nu} \,, \\
\mathcal{O}_{T_2}^g &\equiv \frac{1}{M^2}\phi i\partial^\mu i\partial^\nu \phi \mathcal{O}^g_{\mu\nu} \ .
\end{aligned} \tag{3.2}$$

Note that there is no spin-dependent interactions in the case of scalar boson DM.

3.2 Wilson coefficients

We next discuss the matching condition for the Wilson coefficients of the above operators in a theory where the interactions of the scalar boson with quarks are given by

$$\mathcal{L} = \overline{\psi}_q (a_q + b_q\gamma_5) q\phi + \text{h.c.} \,, \tag{3.3}$$

JHEP05(2015)037

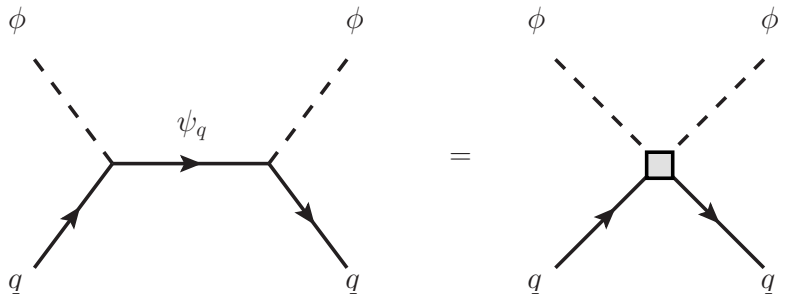

Figure 3. Tree-level matching condition for scalar boson-quark effective interactions. Gray square represents the vertex for the quark effective operators.

where ψ_q denotes a colored fermion with a mass of M_{ψ_q}. Then, with the tree-level matching procedure for the WIMP-quark interactions illustrated in figure 3, we obtain

$$C_S^q(\mu_F) = \frac{a_q^2 + b_q^2}{2} \frac{2M_{\psi_q}^2 - M^2}{(M_{\psi_q}^2 - M^2)^2} + \frac{a_q^2 - b_q^2}{m_q} \frac{M_{\psi_q}}{M_{\psi_q}^2 - M^2} \,, \tag{3.4}$$

$$C_{T_2}^q(\mu_F) = \frac{2(a_q^2 + b_q^2)M^2}{(M_{\psi_q}^2 - M^2)^2} \,. \tag{3.5}$$

Again, the calculation is valid only when the mass difference between the heavy mediator particle and the real scalar boson is much larger than the energy of external quarks. The matching condition for the gluon operators is, on the other hand, obtained through the procedure shown in figure 4. We have

$$C_S^g(\mu_F) = \sum_q \frac{a_q^2 + b_q^2}{12(M_{\psi_q}^2 - M^2)} \,, \tag{3.6}$$

$$C_{T_2}^g(\mu_F) = 0 \,. \tag{3.7}$$

Further, in appendix, we give a result for the loop-computation of the one-loop diagrams in the left-hand side in figure 4, since as far as we know there has been no such a calculation in the literature. The result is useful for the cases where the masses of the colored particles are not so heavy compared with some of the quark masses.

3.3 Scattering cross sections

We now ready to evaluate the scattering cross section of the real scalar boson with a target nucleus. The spin-independent coupling of the real scalar boson with a nucleon defined by

$$\mathcal{L}_{\rm SI}^{(N)} = f_N \phi^2 \overline{N} N \,, \tag{3.8}$$

is evaluated as

$$\begin{aligned} f_N/m_N = \sum_{q=u,d,s} C_S^q(\mu_{\rm had}) f_{T_q}^{(N)} - \frac{8}{9} C_S^g(\mu_{\rm had}) f_{T_G}^{(N)} \\ + \frac{3}{4} \sum_q^{N_f} C_{T_2}^q(\mu) [q(2;\mu) + \overline{q}(2;\mu)] - \frac{3}{4} C_{T_2}^g(\mu) g(2;\mu) \,. \end{aligned} \tag{3.9}$$

JHEP05(2015)037

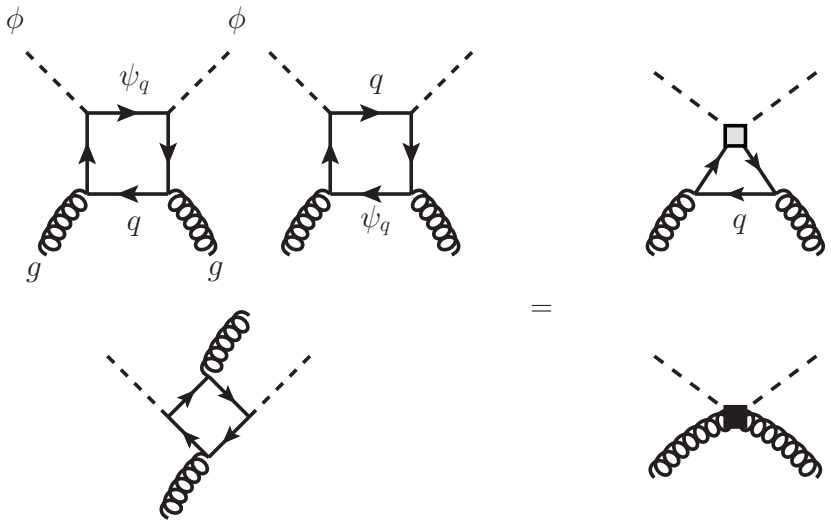

Figure 4. One-loop matching condition for scalar boson-gluon effective interactions. Black square represents the vertex for the gluon effective operators.

In the scalar boson case, there is no spin-dependent coupling with a nucleon. By using the effective coupling, we calculate the scattering cross section of the real scalar boson with a target nucleus as follows:

$$\sigma = \frac{1}{\pi}\left(\frac{M_T}{M+M_T}\right)^2 |n_p f_p + n_n f_n|^2 \,. \tag{3.10}$$

4 Formalism: real vector boson DM

Finally, we consider real vector boson DM. For previous calculation, see ref. [33] and references therein.

4.1 Effective Lagrangian

The effective interactions of the real vector boson B_μ with quarks and gluon are written as

$$\mathcal{L}_{\rm eff} = \sum_{p=q,g} C_S^p \mathcal{O}_S^p + \sum_{p=q,g} C_{T_2}^p \mathcal{O}_{T_2}^p + \sum_q C_{AV}^q \mathcal{O}_{AV}^q \,, \tag{4.1}$$

with

$$\begin{aligned}
\mathcal{O}_S^q &\equiv B^\mu B_\mu m_q \bar{q} q \,, \\
\mathcal{O}_S^g &\equiv \frac{\alpha_s}{\pi} B^\rho B_\rho G^{A\mu\nu} G^A_{\mu\nu} \,, \\
\mathcal{O}_{T_2}^q &\equiv \frac{1}{M^2} B^\rho i\partial^\mu i\partial^\nu B_\rho \mathcal{O}^q_{\mu\nu} \,, \\
\mathcal{O}_{T_2}^g &\equiv \frac{1}{M^2} B^\rho i\partial^\mu i\partial^\nu B_\rho \mathcal{O}^g_{\mu\nu} \,, \\
\mathcal{O}_{AV}^q &\equiv \frac{1}{M} \epsilon_{\mu\nu\rho\sigma} B^\mu i\partial^\nu B^\rho \bar{q}\gamma^\sigma\gamma_5 q \,,
\end{aligned} \tag{4.2}$$

where $\epsilon^{\mu\nu\rho\sigma}$ is the totally antisymmetric tensor with $\epsilon^{0123} \equiv +1$. Here, the vector boson field is supposed to satisfy the on-shell condition $(\Box + M^2)B_\mu = 0$ and $\partial_\mu B^\mu = 0$.

JHEP05(2015)037

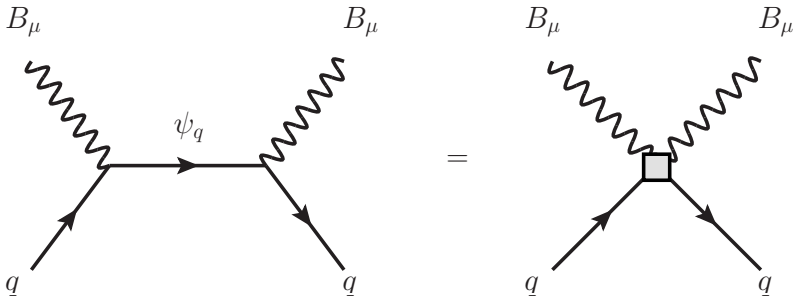

Figure 5. Tree-level matching condition for vector boson-quark effective interactions. Gray square represents the vertex for the quark effective operators.

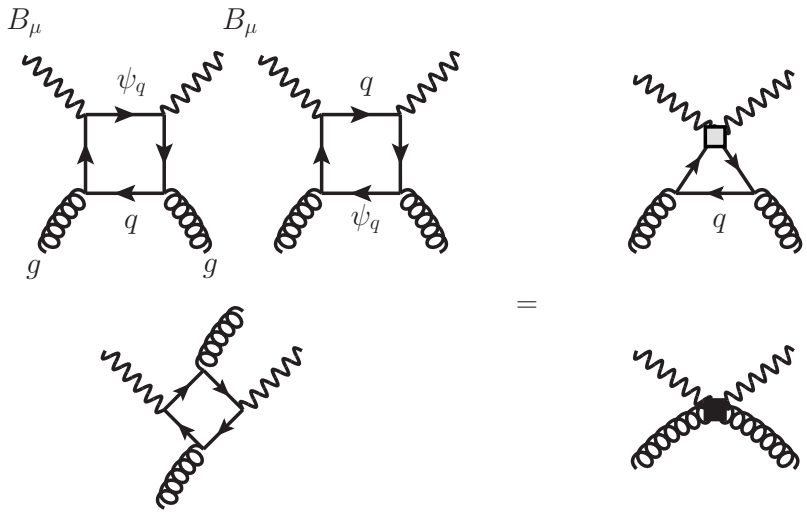

Figure 6. One-loop matching condition for vector boson-gluon effective interactions. Black square represents the vertex for the gluon effective operators.

4.2 Wilson coefficients

Let us evaluate the Wilson coefficients of the above operators in the presence of a fermionic colored particle ψ_q coupling to the WIMP and quarks through the interactions:

$$\mathcal{L} = \overline{\psi}_q(a_q\gamma^\mu + b_q\gamma^\mu\gamma_5)qB_\mu + \text{h.c.}\,. \tag{4.3}$$

In this case, figure 5 yields the matching condition for the WIMP-quark effective couplings as

$$C_S^q(\mu_F) = -(a_q^2+b_q^2)\frac{M_{\psi_q}^2}{2(M_{\psi_q}^2-M^2)^2} + \frac{a_q^2-b_q^2}{m_q}\frac{M_{\psi_q}}{M_{\psi_q}^2-M^2}\,, \tag{4.4}$$

$$C_{T_2}^q(\mu_F) = -\frac{2(a_q^2+b_q^2)M^2}{(M_{\psi_q}^2-M^2)^2}\,, \tag{4.5}$$

$$C_{AV}^q(\mu_F) = \frac{i(a_q^2+b_q^2)M}{M_{\psi_q}^2-M^2}\,. \tag{4.6}$$

JHEP05(2015)037

As for the gluon contribution, figure 6 reads

$$C_S^g(\mu_F) = \sum_q \frac{a_q^2 + b_q^2}{12(M_{\psi_q}^2 - M^2)} \,, \tag{4.7}$$

$$C_{T_2}^g(\mu_F) = 0 \,. \tag{4.8}$$

4.3 Scattering cross sections

By using the results obtained above, we now evaluate the spin-independent WIMP-nucleon coupling. With the definition

$$\mathcal{L}_{\rm SI}^{(N)} = f_N B_\mu B^\mu \overline{N} N \,, \tag{4.9}$$

we have

$$\begin{aligned} f_N/m_N = &\sum_{q=u,d,s} C_S^q(\mu_{\rm had}) f_{T_q}^{(N)} - \frac{8}{9} C_S^g(\mu_{\rm had}) f_{T_G}^{(N)} \\ &+ \frac{3}{4} \sum_q^{N_f} C_{T_2}^q(\mu)[q(2;\mu) + \overline{q}(2;\mu)] - \frac{3}{4} C_{T_2}^g(\mu) g(2;\mu) \,. \end{aligned} \tag{4.10}$$

On the other hand, the spin-dependent effective coupling is given by

$$\mathcal{L}_{\rm SD}^{(N)} = \frac{a_N}{M} \epsilon_{\mu\nu\rho\sigma} B^\mu i\partial^\nu B^\rho \overline{N} \gamma^\sigma \gamma_5 N \,, \tag{4.11}$$

where

$$a_N = \sum_{q=u,d,s} C_{AV}^q \Delta q_N \,. \tag{4.12}$$

With these effective couplings, we eventually get the scattering cross section of the real vector boson with a target nucleus as

$$\sigma = \frac{1}{\pi} \left(\frac{M_T}{M + M_T} \right)^2 \left[|n_p f_p + n_n f_n|^2 + \frac{8}{3} \frac{J+1}{J} |a_p \langle s_p \rangle + a_n \langle s_n \rangle|^2 \right] \,. \tag{4.13}$$

5 Analysis

Now we apply our formulation to a concrete DM model, and discuss the renormalization effects on the calculation. Here, we consider a Majorana fermion interacting with only the third generation right-handed quarks with a unit coupling constant; i.e., $a_q = b_q = 0$ for $q = u, d, s, c$ and $a_q = b_q = 1/2$ for $q = b, t$ in eq. (2.13). Since the new colored scalar particles introduced to the scenario only couple to the third generation quarks, the LHC constraints on them are less severe compared with those interacting with the first two generation quarks. This model is a simplified model for a system composed of a neutralino DM and a pair of right-handed stop and sbottom in the MSSM, though the couplings between them are different from above assumption.

By using the model, we first discuss the scale at which we evaluate the nucleon matrix elements of the twist-2 operators. As mentioned in section 2.2, the twist-2 operators are not

JHEP05(2015)037

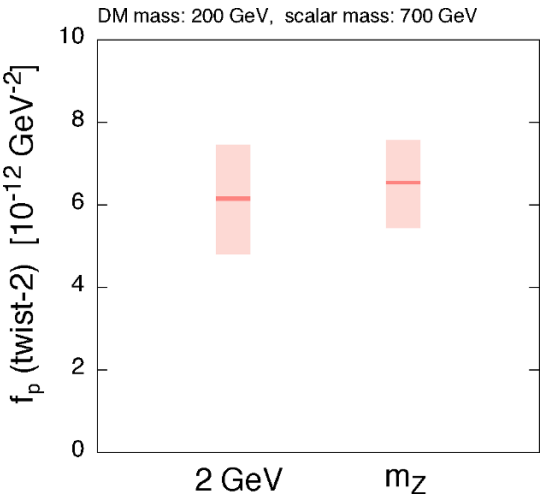

Figure 7. Comparison of twist-2 contributions to WIMP-proton effective coupling calculated with PDFs obtained at $\mu = 2\,\mathrm{GeV}$ and m_Z. Here, we assume the WIMP is a Majorana fermion coupled with right-handed t- and b-quarks (see text), and we take $M = 200\,\mathrm{GeV}$ and $M_{\tilde{q}} = 700\,\mathrm{GeV}$. Red (light-pink) bar denotes the uncertainty coming from the PDF input (perturbation in α_s).

mixed with the scalar-type and axial-vector operators so that we may take a scale for the matrix elements of the twist-2 operators which is different from that of the other ones, and the matrix elements are obtained in a wide range of energy scales. Thus, it is important to determine which scale is appropriate for the calculation of the twist-2 contribution. In figure 7, we compare the twist-2 contributions to the WIMP-proton effective coupling,

$$f_p\ (\text{twist-2})/m_p = \frac{3}{4}\sum_{q}^{N_f}\sum_{i=1,2} C_{T_i}^{q}(\mu)[q(2;\mu)+\overline{q}(2;\mu)] - \frac{3}{4}\sum_{i=1,2} C_{T_i}^{g}(\mu) g(2;\mu)\,, \tag{5.1}$$

evaluated with the PDFs obtained at $\mu = 2\,\mathrm{GeV}$ and m_Z. Here, we take $M = 200\,\mathrm{GeV}$ and $M_{\tilde{q}} = 700\,\mathrm{GeV}$. The red (light-pink) bar denotes the uncertainty coming from the PDF input (perturbation in α_s). For the estimation of the uncertainty from the PDF error, we follow the method described in ref. [16] with the χ^2 tolerance T taken to be $T = 10$. The uncertainty caused by the neglect of the higher-order contribution in α_s is evaluated by varying the input and quark-mass threshold scales by a factor of two, i.e., $M_{\tilde{q}}/2 \le \mu_F \le 2M_{\tilde{q}}$, $m_t/2 \le \mu_t \le 2m_t$, and so on. It turns out that both calculations predict similar values for the twist-2 contribution, though the theoretical error in the case of $\mu = 2\,\mathrm{GeV}$ is a little bit larger than that with $\mu = m_Z$. If one sets $\mu = 1\,\mathrm{GeV}$, we expect that the error becomes much larger due to the charm-quark threshold effects since in the low-energy region the strong coupling constant rapidly grows up. In addition, the higher-dimensional operators suppressed by a power of the quark masses may give significant contribution if the scale μ is taken to be at a low-energy scale as discussed in section 2.5, which also contribute to the theoretical uncertainty. For these reasons, we conclude that it is appropriate to set the PDF scale μ in a high-scale region, not the hadronic scale. In the following calculation, we take the scale to be $\mu = m_Z$.

JHEP05(2015)037

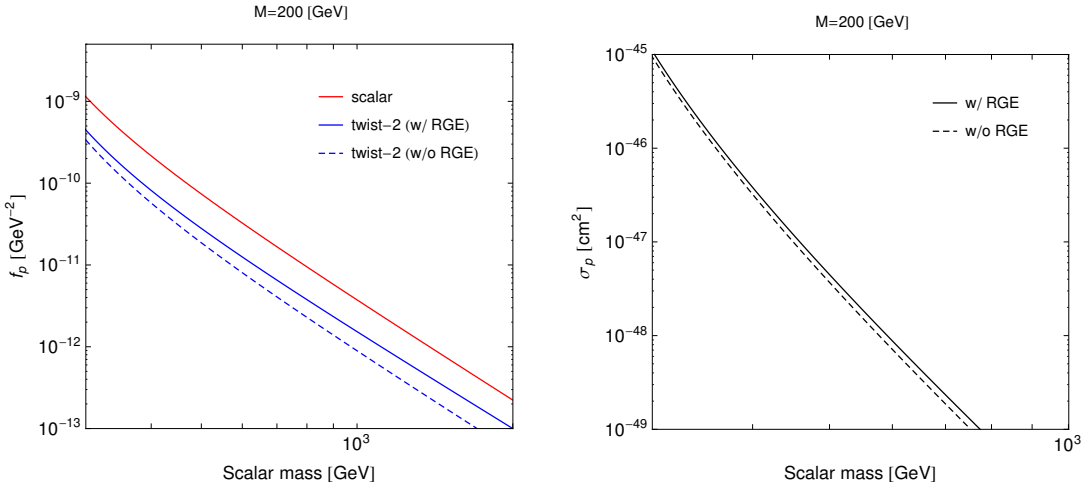

(a) Effective coupling f_p

(b) Scattering cross section σ_p

Figure 8. (a) Each contribution to the WIMP-proton effective coupling f_p as functions of the mediator mass $M_{\tilde{q}}$. DM model adopted here is the same as figure 7. Upper red (lower blue) line shows the contribution of the scalar-type (twist-2-type) operators. For the twist-2 contribution, solid and dashed lines show the results with and without the renormalization effects, respectively. (b) WIMP-proton scattering cross section σ_p as a function of $M_{\tilde{q}}$. Solid and dashed lines show the results with and without the renormalization effects, respectively. In both plots, WIMP mass is set to be $M = 200\,\mathrm{GeV}$.

Next, we show the renormalization effects on the WIMP-nucleon scattering. As discussed in section 2.4, the twist-2 operators receive the renormalization effects. The effects are expected to be significant when the input scale μ_F, i.e., the typical mass scale of colored mediators, is much higher than the electroweak scale.

In figure 8(a), we show each contribution to the WIMP-proton effective coupling f_p as functions of the mediator mass $M_{\tilde{q}}$. We set the WIMP mass to be $M = 200\,\mathrm{GeV}$. The upper red (lower blue) line shows the contribution of the scalar-type (twist-2-type) operators. For the twist-2 contribution, we show both calculations with and without the renormalization effects in solid and dashed lines, respectively. By using the effective coupling, we then evaluate the WIMP-proton scattering cross section σ_p. We plot it as a function of $M_{\tilde{q}}$ in figure 8(b). Here again the WIMP mass is set to be $M = 200\,\mathrm{GeV}$. The solid and dashed lines show the results with and without the renormalization effects, respectively. We find that the renormalization effects change the resultant value for the twist-2 contribution by more than 50% when $M_{\tilde{q}} \gtrsim 500\,\mathrm{GeV}$. In this case, the scattering cross sections are modified by more than 20%. The results indicate that it is important to include the RGE effects, especially when the colored mediators are much heavier than the electroweak scale.

6 Conclusion and discussion

So far we have discussed a way of evaluating the WIMP-nucleon scattering cross section at the leading order in α_s based on the effective theoretical approach. We have considered a Majorana fermion, real scalar and vector bosons, and presented formulation for each case.

JHEP05(2015)037

Further, using a particular example with a Majorana fermion, we have shown that the renormalization effects may change the twist-2 contribution by more than 50% when the colored mediators are much heavier than the electroweak scale, which results in modification to the WIMP-nucleon scattering cross section by $\mathcal{O}(10)\%$.

As shown in figure 7, the calculation of the twist-2 contribution suffers from $\mathcal{O}(10)\%$ uncertainty due to the perturbation in α_s. It is possible to reduce the uncertainty by going beyond the leading-order calculation. In fact, we have already had the higher-order results for the RGEs and the matching conditions at each quark threshold, as commented in section 2.4. To complete the next-to-leading order computation, however, we further need the higher-order matching conditions between the full and effective theories at the input scale. We defer the calculation as future work. In addition, we expect that future lattice QCD simulations will much improve the determination of the quark content in nucleon. These two developments will enable us to evaluate the WIMP-nucleon scattering cross sections with great accuracy.

Finally, we would like to emphasize that the prescription for the computation of the WIMP-nucleon scattering cross section discussed in this paper is quite systematic, and the formulation itself is almost model-independent. The model-dependence is included in the Wilson coefficients at the factorization scale, and the subsequent procedure is similar in every case. Therefore, this method is suitable to be used in general computational codes for the direct detection rate of DM, such as `micrOMEGAs` [5] and `DarkSUSY` [6].

Acknowledgments

The work of J.H. is supported by Grant-in-Aid for Scientific research from the Ministry of Education, Science, Sports, and Culture (MEXT), Japan, No. 24340047 and No. 23104011, and also by World Premier International Research Center Initiative (WPI Initiative), MEXT, Japan. The work of R.N. and N.N. is supported by Research Fellowships of the Japan Society for the Promotion of Science for Young Scientists, No. 26·3947 (R.N.) and No. 26·8296 (N.N.).

A Gluon-loop contribution for real scalar boson DM

In this appendix, we give a result for the calculation of one-loop gluon contribution in the case of real scalar boson DM, with quark masses kept non-vanishing. Similar results have been already obtained for the cases of Majorana fermion and real vector boson in refs. [4] and [33], respectively.

We assume that the interactions of the real scalar boson with quarks and the corresponding colored heavy fermions are described in terms of the Lagrangian given in eq. (3.3). The diagrams we consider here are illustrated in figure 9. By evaluating the diagrams, we compute the contribution of a heavy quark Q to the coefficient of the gluon scalar-type operator C_S^g as

$$C_S^g|_Q = \frac{1}{4} \sum_{i=a,b,c} \left[(a_Q^2 + b_Q^2) f_+^{(i)}(M; m_Q, m_{\psi_Q}) + (a_Q^2 - b_Q^2) f_-^{(i)}(M; m_Q, m_{\psi_Q}) \right] , \quad \text{(A.1)}$$

JHEP05(2015)037

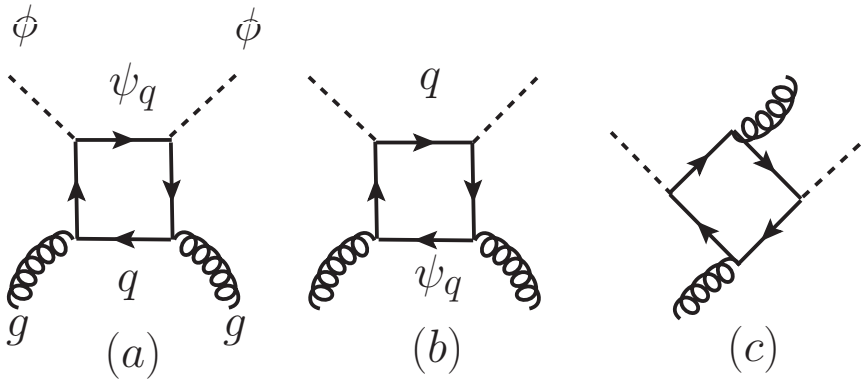

Figure 9. One-loop contribution to the WIMP-gluon coupling.

where $f_+^{(i)}$ and $f_-^{(i)}$ $(i = a, b, c)$ correspond to the contribution of the diagram (i) in figure 9. They are given as follows:

$$f_+^{(a)}(M; m_1, m_2) \equiv -\frac{m_1^2 m_2^4 (M^2 + m_1^2 - m_2^2)}{\Delta^2} L - \frac{(-M^2 + m_1^2 + 2m_2^2)\Delta + 6m_1^2 m_2^2 (M^2 - m_1^2 + m_2^2)}{6\Delta^2}, \tag{A.2}$$

$$f_-^{(a)}(M; m_1, m_2) \equiv \frac{m_1 m_2^3 \{\Delta + m_1^2 (M^2 - m_1^2 + m_2^2)\}}{\Delta^2} L - \frac{m_2 \{(-2M^2 + m_1^2 + 2m_2^2)\Delta - 6m_1^2 m_2^2 (M^2 + m_1^2 - m_2^2)\}}{6m_1 \Delta^2}, \tag{A.3}$$

$$f_+^{(b)}(M; m_1, m_2) \equiv f_+^{(a)}(M; m_2, m_1), \tag{A.4}$$

$$f_-^{(b)}(M; m_1, m_2) \equiv f_-^{(a)}(M; m_2, m_1), \tag{A.5}$$

$$f_+^{(c)}(M; m_1, m_2) \equiv \frac{-M^2 + m_1^2 + m_2^2}{2\Delta} - \frac{m_1^2 m_2^2}{\Delta} L, \tag{A.6}$$

$$f_-^{(c)}(M; m_1, m_2) \equiv \frac{2m_1 m_2}{\Delta} - \frac{m_1 m_2 (-M^2 + m_1^2 + m_2^2)}{\Delta} L, \tag{A.7}$$

with

$$\Delta(M; m_1, m_2) \equiv M^4 - 2M^2 (m_1^2 + m_2^2) + (m_2^2 - m_1^2)^2, \tag{A.8}$$

$$L(M; m_1, m_2) \equiv \begin{cases} \dfrac{1}{\sqrt{|\Delta|}} \ln \left(\dfrac{m_1^2 + m_2^2 - M^2 + \sqrt{|\Delta|}}{m_1^2 + m_2^2 - M^2 - \sqrt{|\Delta|}} \right) & (\Delta > 0) \\ \dfrac{2}{\sqrt{|\Delta|}} \arctan \left(\dfrac{\sqrt{|\Delta|}}{m_1^2 + m_2^2 - M^2} \right) & (\Delta < 0) \end{cases}. \tag{A.9}$$

JHEP05(2015)037

In particular, if $m_1 \ll M, m_2$, the above functions are approximated by

$$
\begin{aligned}
f_+^{(a)} &\simeq -\frac{2m_2^2 - M^2}{6(m_2^2 - M^2)^2}\,, \\
f_-^{(a)} &\simeq -\frac{m_2}{3m_1(m_2^2 - M^2)}\,, \\
f_+^{(b)} &\simeq -\frac{1}{6(m_2^2 - M^2)}\,, \\
f_-^{(b)} &\simeq 0\,, \\
f_+^{(c)} &\simeq \frac{1}{2(m_2^2 - M^2)}\,, \\
f_-^{(c)} &\simeq 0\,.
\end{aligned}
\tag{A.10}
$$

By using the expressions and the tree-level result in eq. (3.4), one readily obtains the matching condition (3.7).

Open Access. This article is distributed under the terms of the Creative Commons Attribution License (CC-BY 4.0), which permits any use, distribution and reproduction in any medium, provided the original author(s) and source are credited.

References

[1] Planck collaboration, P.A.R. Ade et al., *Planck 2013 results. XVI. Cosmological parameters*, *Astron. Astrophys.* **571** (2014) A16 [arXiv:1303.5076] [INSPIRE].

[2] LUX collaboration, D.S. Akerib et al., *First results from the LUX dark matter experiment at the Sanford Underground Research Facility*, *Phys. Rev. Lett.* **112** (2014) 091303 [arXiv:1310.8214] [INSPIRE].

[3] M. Drees and M. Nojiri, *Neutralino-nucleon scattering revisited*, *Phys. Rev.* **D 48** (1993) 3483 [hep-ph/9307208] [INSPIRE].

[4] J. Hisano, K. Ishiwata and N. Nagata, *Gluon contribution to the dark matter direct detection*, *Phys. Rev.* **D 82** (2010) 115007 [arXiv:1007.2601] [INSPIRE].

[5] G. Bélanger, F. Boudjema, A. Pukhov and A. Semenov, *MicrOMEGAs_3: a program for calculating dark matter observables*, *Comput. Phys. Commun.* **185** (2014) 960 [arXiv:1305.0237] [INSPIRE].

[6] P. Gondolo et al., *DarkSUSY: computing supersymmetric dark matter properties numerically*, *JCAP* **07** (2004) 008 [astro-ph/0406204] [INSPIRE].

[7] G. Jungman, M. Kamionkowski and K. Griest, *Supersymmetric dark matter*, *Phys. Rept.* **267** (1996) 195 [hep-ph/9506380] [INSPIRE].

[8] H.D. Politzer, *Power corrections at short distances*, *Nucl. Phys.* **B 172** (1980) 349 [INSPIRE].

[9] C. Arzt, *Reduced effective Lagrangians*, *Phys. Lett.* **B 342** (1995) 189 [hep-ph/9304230] [INSPIRE].

[10] A.J. Buras, *Asymptotic freedom in deep inelastic processes in the leading order and beyond*, *Rev. Mod. Phys.* **52** (1980) 199 [INSPIRE].

JHEP05(2015)037

[11] P. Gondolo and S. Scopel, *On the sbottom resonance in dark matter scattering*, *JCAP* **10** (2013) 032 [arXiv:1307.4481] [INSPIRE].

[12] J. Hisano, K. Ishiwata and N. Nagata, *Direct search of dark matter in high-scale supersymmetry*, *Phys. Rev.* **D 87** (2013) 035020 [arXiv:1210.5985] [INSPIRE].

[13] R.D. Young and A.W. Thomas, *Octet baryon masses and sigma terms from an* SU(3) *chiral extrapolation*, *Phys. Rev.* **D 81** (2010) 014503 [arXiv:0901.3310] [INSPIRE].

[14] JLQCD collaboration, H. Ohki et al., *Nucleon strange quark content from $N_f = 2 + 1$ lattice QCD with exact chiral symmetry*, *Phys. Rev.* **D 87** (2013) 034509 [arXiv:1208.4185] [INSPIRE].

[15] M.A. Shifman, A.I. Vainshtein and V.I. Zakharov, *Remarks on Higgs boson interactions with nucleons*, *Phys. Lett.* **B 78** (1978) 443 [INSPIRE].

[16] J.F. Owens, A. Accardi and W. Melnitchouk, *Global parton distributions with nuclear and finite-Q^2 corrections*, *Phys. Rev.* **D 87** (2013) 094012 [arXiv:1212.1702] [INSPIRE].

[17] SPIN MUON collaboration, D. Adams et al., *A New measurement of the spin dependent structure function $g1(x)$ of the deuteron*, *Phys. Lett.* **B 357** (1995) 248 [INSPIRE].

[18] J. Hisano, K. Ishiwata and N. Nagata, *Direct detection of dark matter degenerate with colored particles in mass*, *Phys. Lett.* **B 706** (2011) 208 [arXiv:1110.3719] [INSPIRE].

[19] J. Hisano, K. Ishiwata and N. Nagata, *A complete calculation for direct detection of Wino dark matter*, *Phys. Lett.* **B 690** (2010) 311 [arXiv:1004.4090] [INSPIRE].

[20] R.J. Hill and M.P. Solon, *Universal behavior in the scattering of heavy, weakly interacting dark matter on nuclear targets*, *Phys. Lett.* **B 707** (2012) 539 [arXiv:1111.0016] [INSPIRE].

[21] R.J. Hill and M.P. Solon, *Standard model anatomy of WIMP dark matter direct detection II: QCD analysis and hadronic matrix elements*, *Phys. Rev.* **D 91** (2015) 043505 [arXiv:1409.8290] [INSPIRE].

[22] T. van Ritbergen, J.A.M. Vermaseren and S.A. Larin, *The four loop β-function in quantum chromodynamics*, *Phys. Lett.* **B 400** (1997) 379 [hep-ph/9701390] [INSPIRE].

[23] M. Czakon, *The four-loop QCD β-function and anomalous dimensions*, *Nucl. Phys.* **B 710** (2005) 485 [hep-ph/0411261] [INSPIRE].

[24] K.G. Chetyrkin, *Quark mass anomalous dimension to $O(\alpha_S^4)$*, *Phys. Lett.* **B 404** (1997) 161 [hep-ph/9703278] [INSPIRE].

[25] J.A.M. Vermaseren, S.A. Larin and T. van Ritbergen, *The four loop quark mass anomalous dimension and the invariant quark mass*, *Phys. Lett.* **B 405** (1997) 327 [hep-ph/9703284] [INSPIRE].

[26] D.J. Gross and F. Wilczek, *Asymptotically free gauge theories. 2*, *Phys. Rev.* **D 9** (1974) 980 [INSPIRE].

[27] A. Vogt, S. Moch and J.A.M. Vermaseren, *The three-loop splitting functions in QCD: the singlet case*, *Nucl. Phys.* **B 691** (2004) 129 [hep-ph/0404111] [INSPIRE].

[28] S.A. Larin, *The renormalization of the axial anomaly in dimensional regularization*, *Phys. Lett.* **B 303** (1993) 113 [hep-ph/9302240] [INSPIRE].

[29] A. Djouadi and M. Drees, *QCD corrections to neutralino nucleon scattering*, *Phys. Lett.* **B 484** (2000) 183 [hep-ph/0004205] [INSPIRE].

JHEP05(2015)037

[30] P.L. Cho and E.H. Simmons, *Searching for G3 in $t\bar{t}$ production*, *Phys. Rev.* **D 51** (1995) 2360 [hep-ph/9408206] [INSPIRE].

[31] L. Vecchi, *WIMPs and un-naturalness*, arXiv:1312.5695 [INSPIRE].

[32] ETM collaboration, S. Dinter et al., *Sigma terms and strangeness content of the nucleon with $N_f = 2 + 1 + 1$ twisted mass fermions*, *JHEP* **08** (2012) 037 [arXiv:1202.1480] [INSPIRE].

[33] J. Hisano, K. Ishiwata, N. Nagata and M. Yamanaka, *Direct detection of vector dark matter*, *Prog. Theor. Phys.* **126** (2011) 435 [arXiv:1012.5455] [INSPIRE].

JHEP05(2015)037